ROBOT-BASED RESEARCH ON THREE-LAYER ORIENTED FLAKEBOARDS

Kaiyuan Wang
Graduate Research Assistant

and

Frank Lam
Assistant Professor

Department of Wood Science
Faculty of Forestry
University of British Columbia
#389-2357 Main Mall
Vancouver, BC, Canada V6T 1Z4

(Received August 1997)

ABSTRACT

A small jointed-arm motion type robot system was introduced for wood mat formation to study the relationship between wood mat structure and panel properties. Four types of structures of three-layer oriented flakeboards with different face to core ratios and core orientations were formed using the robot as a tool. The panels were then hot-pressed and tested for horizontal density distribution (HDD) by X-ray machine, bending modulus of elasticity (MOE), internal bond (IB) and thickness swelling (TS). The results showed that the programmed robot formed panels with well-defined and reproducible structures. Linked with the existing panel simulation program, X-ray data, and real properties, the panel structure with face to core ratio of 15:70:15 and random core has been considered the most suitable panel pattern for additional research based on its superior performance and lower variation of properties.

Keywords: robot, structure, property, density distribution, simulation, X-ray.

INTRODUCTION

For short-fiber wood composites, it is well accepted that the organization of short-fiber wood elements has strong influence on the properties of the composite mat. Such packing behavior of the wood elements controls the degree of wood element contact and horizontal density distribution (HDD) of the composite mat. The HDD and the vertical density distribution of flakeboards are two important factors when studying the relationships between processing parameters and panel properties. Recently, significant progress has been made to apply geometric probability theory to determine the randomly formed flakeboard structure and corresponding mathematical models to study HDD (Suchsland and Xu 1991; Dai and Steiner 1994, Lang and Wolcott 1996). Horizontal density distribution was also quantified, based on a density variation phenomenon and statistical considerations (Xu and Steiner 1995). However, the influence of wood element size, geometry, and deposition factors (such as flake orientation) on the spatial arrangement of wood elements in flakeboards and the influence of flakeboard structure on performance properties are still not fully understood (Kelly 1977). More research is needed to incorporate these variables into the existing models.

A user-friendly simulation program *MAT* was written based on the mathematical model and simulation program developed by Dai and Steiner (Lu 1995). After inputting sufficient variables, this program calculates density variation along the horizontal plane of a simulated

Wood and Fiber Science, 30(4), 1998, pp. 339–347

mat based on different sampling zone size. The position and orientation of each "flake" in the simulated mat are available, yielding a record of the structure of the simulated mat. In order to verify and apply the model, a robot mat formation system was used to manufacture small composite mats (250 mm × 250 mm) with various types of predefined structure determined by the *MAT* simulation program. The philosophy to use a robot mat formation system is that it can act as a tool to link the simulated mat with the real experimental mat. The programmed robot carries out the predefined task—pickup and deposition of thousands of flakes with controlled location and orientation to form flakeboards with high repeatability and accuracy. The method reduces the number of replicates needed for experiments, besides reducing labor costs and saving time.

This study was the first to combine a robot system with experimental design to investigate the organization of wood elements in composite mats. The objectives of this paper were:

(1) To verify the performance of the robot system by evaluating the X-ray scanning density data, computer simulation program, and real density data obtained by gravimetric method of the formed mats;
(2) To develop a database on the physical and mechanical properties as well as HDD of three-layer oriented flakeboards, and to select a suitable mat structure from the four predefined structures for further research.

MATERIALS AND METHODS

Materials

This study consisted of four kinds of three-layer oriented flakeboards formed with different core structure and face to core ratio. Aspen flakes (*Populus tremuloides,* density 0.405 g/cm^3 based on the oven-dry wood weight) were used with average flake size of 75.04 mm × 19.07 mm × 0.61 mm (length × width × thickness).

Laboratory flakes were cut with a disc flaker. The flakes with good shapes and flat surfaces were selected and air-dried for a week before being gently dried in a laboratory oven at temperatures of 60°C for 2 h to maintain the flatness of particles. The dried flakes were stored in plastic bags. The equilibrium moisture content of final dried flakes was approximately 6 to 7% before being measured and placed into a mat.

Phenol-formaldehyde powder resin CASCOPHEN W91B, 6% (based on the oven-dry wood weight) was used in the experiment. The relatively high 6% resin level was selected to ensure full resin coverage on the flakes and compensate for resin lost during the flake blending and mat forming stage using robot technology. Pilot research verified the reliability of using this resin level. Finally, no wax was added.

Blended flakes were deposited into mats by the robot system and then hot-pressed at 180°C to 10-mm stop using 0.8 min closing time, 5 min at stops and 0.5 min decompression by a computer-controlled 300- × 300-mm hot-press (Wabash 27,000 kg load). Preliminary experiments were established to select the above pressing parameters to ensure proper bonding within each kind of mat. Target board density was designed as 0.6 g/cm^3 (based on the calculation from the simulation program with the mat size 250 bmm × 250 mm). The actual averaged board density was 0.587 g/cm^3, based on weight and volume at approximately 9% moisture content. Target mat size was designed as 250 mm × 250 mm × 10 mm (length × width × thickness). The actual averaged mat size was 250 mm × 250 mm × 10.6 mm. General mat structure was three-layer, with face and bottom orientation 0° (target coordinate and actual) and random or cross-aligned core.

Experiment design

A two by two factorial experiment with completely randomized design was employed in this study. The two factors were core orientation (random, R; cross aligned, X) and face to core ratio (30%:70%:50%:50%). These

four combinations of panel structure were referred to in the test as R30, R50, X30, and X50. Three replicates were applied to each type of structure. In each structure type, the orientation and position of the flakes in the three replicates were identical.

Testing method

X-ray scanning method.—After 12 boards were formed and hot-pressed, they were conditioned at 20°C, 65% relative humidity (RH) for two weeks. Afterwards they were cut into the size of 250 mm × 250 mm, and the HDD of each panel was examined by using X-ray densitometry to obtain density data with resolution of 2 mm (in X-direction) and 1.5 mm (in Y-direction).

The point normalized density (point relative density divided by global panel relative density) profile of each mat generated from simulated data and X-ray scanning data was obtained. Here relative density refers to the raw X-ray data that were processed by using curve-fitting algorithms. A linear relationship exists between relative density and real panel density. Global panel density refers to the average density of the whole scanning area, size of 160 mm × 240 mm. A more detailed study was performed by using a sampling zone size of 40 mm × 40 mm to quantify the density variation of robot-formed experimental mats and simulated mat. The scanning area on a mat was divided into 24 small zones. The scanning area and each 40 mm × 40 mm sampling zone position on a panel are shown in Fig. 1. Within a sampling zone, small 2.0-mm × 1.5-mm zones were considered as sample points. The average and the standard deviation of the normalized density of each sampling zone (A_i, SD_i) and the global panel (A, SD) were calculated. Then the normalized average density (A_i/A) and normalized standard deviation of density (SD_i/A) of each sampling zone were calculated based on the X-ray density data. The corresponding sampling area in a simulated mat was also determined with the resolution of 2 mm × 2 mm. The normalized average density and standard deviation of sampling zone (size 40 mm × 40 mm) of the simulation density data were also calculated.

Panel properties tests.—The density of the 250-mm × 250-mm panels, based on panel weight and volume at approximately 9% moisture content, was estimated before the panels were cut into 230-mm × 230-mm size to reduce the edge effect on the performance of the panels. The panels were then cut into specimens for the static bending modulus of elasticity (MOE) tests (specimen size: 230 × 40 mm), the internal bond (IB) tests (size: 50 × 50 mm), and the thickness swelling (TS) tests (50 × 50 mm and 40 × 40 mm). The density of each specimen was also estimated before testing. The X-Y coordinate system (defined by the robot mat formation coordinate system) of a panel and the arrangement of the cutting specimens are shown in Fig. 2.

Two kinds of nondestructive bending MOE tests were applied to the bending specimens along the surface flake aligned direction. A Metriguard stress wave timer (Model 239A) was used to measure the stress wave MSW (modulus of elasticity based on stress-wave data) of each specimen. When using this impact-induced stress wave method, the distance and time of the wave transmission were recorded. The formula to relate MSW and density of the specimen (ρ) and the velocity of wave (v) is:

$$MSW = v^2\rho \qquad (1)$$

Then the specimen was tested on an MTS Sintek test machine according to ASTM D 1037-93 standard using load-controlled 3-point testing mode. A span of 200 mm was used due to the limitation of panel size (230 mm × 40 mm × 11 mm). The results obtained from these two methods were recorded and compared. The nondamaged specimen was further cut into four specimens with the size of 40 mm × 40 mm for the thickness swelling tests.

Then IB and TS tests were performed following the CSA Standard Can/CSA-O437.0-93, Standards on OSB and Waferboard (CSA

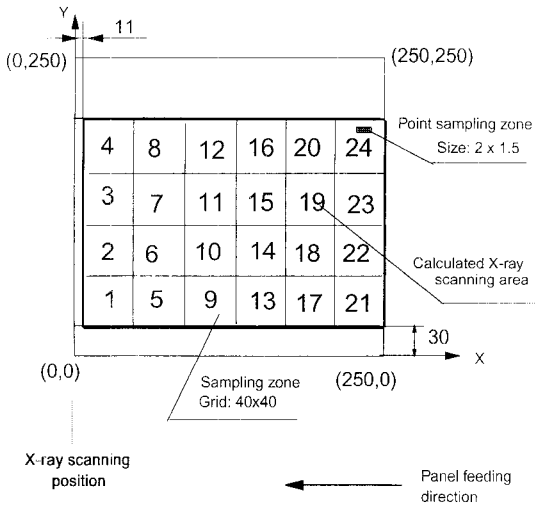

FIG. 1. Sampling zone position in a panel.

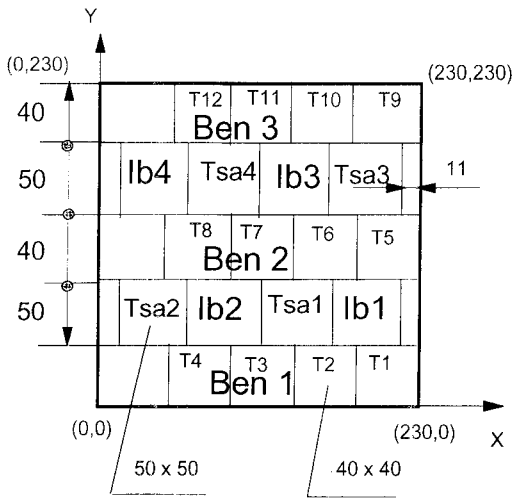

Notes:
all units in mm
Ben refers to specimen for bending tests
Ib refers to specimen for IB tests
T refers to specimen for TS tests with size of 40mm x 40mm
Tsa refers to specimen for TS tests with size of 50mm x 50mm

FIG. 2. Arrangement of specimen cutting.

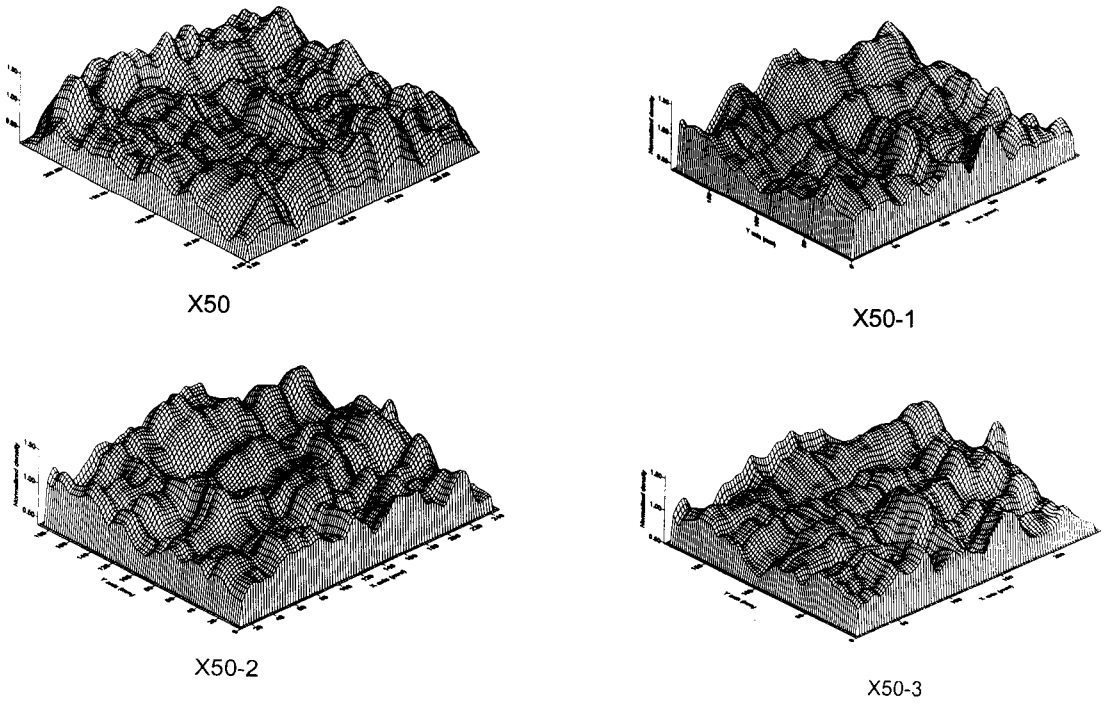

FIG. 3. Normalized density profile of X50 pattern in surface map.

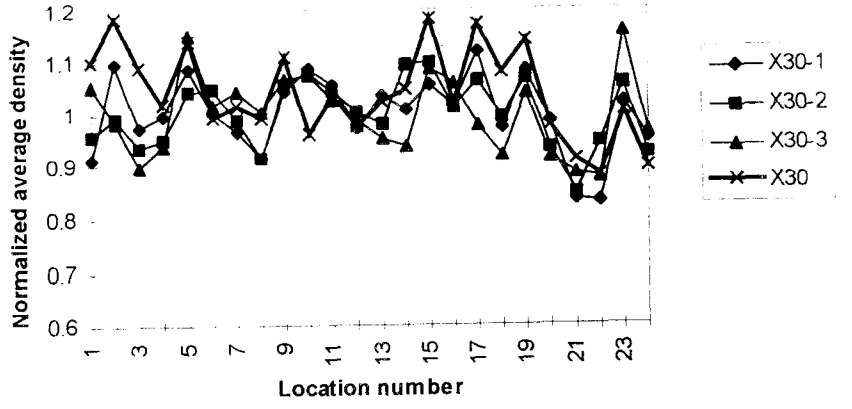

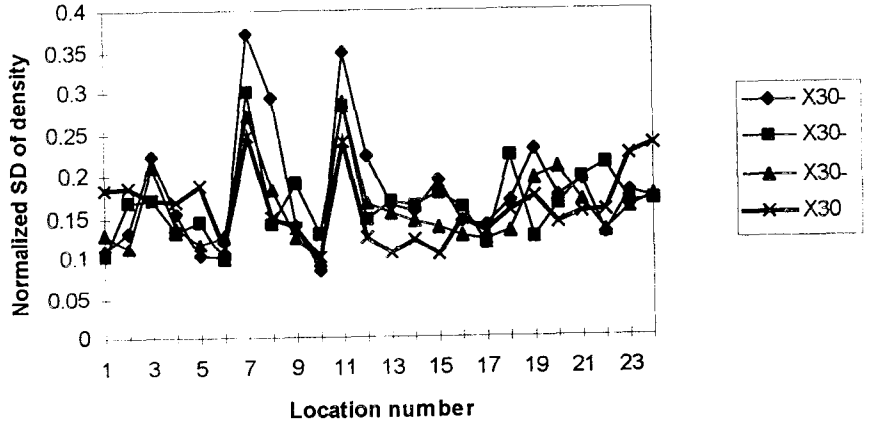

FIG. 4.1. Normalized average sample density of X30 (simulated mat) and X30-1, X30-2 and X30-3 (robot-formed mats). FIG. 4.2. Normalized standard deviation of sample density of X30 (simulated mat) and X30-1, X30-2 and X30-3 (robot-formed mats).

1994). The ultimate strength and the failure position were recorded for each IB sample. Measurement of thickness swelling was tested using a water-soaking method after 24 h at 20°C. The specimen size used was 50 mm × 50 mm or 40 mm × 40 mm instead of standard 150 mm × 150 mm due to the panel size limitation.

RESULTS AND DISCUSSION

Verification of the compatibility of the simulation program and robot mat formation technology

In order to verify the compatibility of the simulation program and robot mat formation

TABLE 1. *Summary of properties of robot-formed oriented strandboard.*

	R30	X30	R50	X50
Bending MOE[a] (MPa)	7,139.8 (8.1)[c]	4,677.1 (13.5)	9,696.7 (15.2)	6,711.2 (30.6)
IB[b] (MPa)	0.553 (11.7)	0.626 (18.2)	0.553 (16.1)	0.711 (23.7)
TS[b] (%)	29.2 (13.2)	26.9 (12.3)	31.0 (8.9)	29.7 (15.6)

[a] MOE: average of 9 specimens using stress-wave method.
[b] IB, TS: average of 12 specimens (size: 50 × 50 mm).
[c] Data in parentheses represent coefficient of variation (%).

TABLE 2. *Summary of analysis of variance for bending MOE, internal bond, and thickness swelling.*

	Source	df	SS	MS	F
Bending MOE (MPa)	A	1	0.223E+08	0.223E+08	33.0*
	B	1	0.158E+08	0.158E+08	23.4*
	A × B	1	2.05E+05	2.05E+05	0.303
	Error	8	5.40E+06	5.40E+06	
	Total	11	0.435E+08		
IB (MPa)	A	1	0.040	0.040	4.24
	B	1	0.005	0.005	0.521
	A × B	1	0.005	0.005	0.532
	Error	8	0.075	0.009	
	Total	11	0.125		
TS (%)	A	1	1.040	1.040	0.177
	B	1	22.05	22.05	3.762
	A × B	1	6.679	6.679	1.139
	Error	8	46.89	5.862	
	Total	11	76.66		

A: core structure (random, perpendicular); B: face to core ratio (30%:70%, 50%:50%).
* Significant with $\alpha = 0.05$.

technology, normalized density profiles generated from the data obtained from the simulation program *MAT* and X-ray scanning machine were compared. Figure 3 shows that the normalized relative density profile of the X50 pattern in surface map where X50 represents simulation panels; and X50-1, X50-2, and X50-3 represent three replicates of the same panel structure scanned by X-ray machine. Figures 4.1 and 4.2 present separately the normalized average and standard deviation of sample density of simulated panel X30 and experimental panels X30-1, X30-2, and X30-3 in 24 different positions in a panel. From the figures, the simulated panel and the robot-formed panels are visually judged to be similar, which provides an indication that the use of the simulation program and robot mat formation technology to analyze the horizontal density distribution in panels is valid. Also Figs. 4.1 and 4.2 show that the three replicates, X30-1, X30-2, and X30-3, have similar density distribution, which demonstrates good repeatability of the robot mat formation system. Such repeatability is also evident in the other three panel structures.

Criteria for selecting a suitable pattern from the four structures

The final testing results of strength and physical properties of robot-formed panels are summarized in Table 1. A summary of analysis of variance (ANOVA) for bending MOE, internal bond, and thickness swelling with variables of core structure and face to core ratio is tabulated in Table 2.

Bending MOE.—The results of two kinds of nondestructive bending MOE tests were calculated and compared in Fig. 5. A good correlation is found with the coefficient of determination $R^2 = 0.72$. It can be summarized

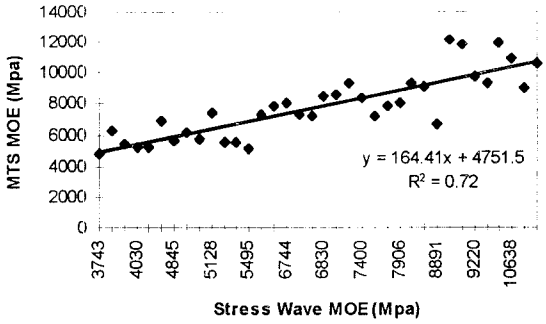

FIG. 5. Relationship between the bending MOE tested by stress wave method and MTS testing machine.

from ANOVA that both core orientation and face to core ratio have great influence on the bending MOE. Combined with the results in Table 1, it can be concluded that the flake alignment in face and core of a board is the strongest factor to influence the MOE property. For a given total number of flakes to form a panel, bending MOE can be improved when more flakes are aligned along the specimens' long axis. This explained why R50 has higher MOE value than X30. The order of MOE by ascending sequence is: X30 → X50 → R30 → R50.

Internal bond.—It is indicated from ANOVA results in Table 2 that IB is neither significantly affected by the core orientation nor by the face to core ratio. This means that IB is not affected by alignment of the flakes, which agrees with the results reported by Geimer (1981) and McNatt et al. (1992). In our experiment, it was found that 75% of the failure positions during IB tests occurred in the middle of the panel thickness, which agrees with the general conclusion that the internal bond strength is weakest near the center of the panel due to relatively poor heat and mass transfer. It can be seen from Table 1 that all four patterns have very good IB performance (higher than the required value listed in the standard CSA0437.0 grade O-2 Span Rated which is 0.345MPa). The order of increasing IB is: R30,R50 → X30 → X50.

Thickness swelling.—Thickness swelling is not significantly affected by either core structure or face to core ratio (See Table 2). In order to get additional data, each specimen used for the bending tests was further cut into four specimens (size: 40 × 40 mm^2) for the thickness swelling tests (Specimen No. T1–T12). Results using the 40-mm × 40-mm specimens were similar to those obtained using the 50-mm × 50-mm specimens (Specimen No. Tsa1–Tsa4). In this experiment, the order of increasing thickness swelling is: X30 → R30 → X50 → R50.

Combining the information obtained from the above analysis, X50 has the largest variation of properties. Rough surfaces along one of the edges parallel to the X-axis can be visually detected in specimen panels X50-1, X50-2 and X50-3, which led to relatively large within-panel density variation as shown in the density profiles from the X-ray data and simulation program (Fig. 3). The resulting HDD density variation further led to high variation of panel properties. Such rough surfaces were not detected in other panel structures. It is also noted that X30 pattern has the lowest bending strength, which is lower than the value of 5,500 MPa required in CSA Standard Can/CSA-O437.0-Grade O-2 Span Rated (CSA 1993). Furthermore, increase of the face/core ratio results in reduced MOE when specimens are tested perpendicular to the face flake alignment (Y-direction) (Avramidis and Smith 1989) and R50 doesn't have superior performances besides bending MOE in X direction. Therefore, the R30 pattern (random core, oriented face, 30%: 70% face to core ratio) is considered most suitable for future study in the research program.

Verification of the repeatability of the panel performance

The repeatability of the panel performance of the three replicates for each structure has been verified by plotting the property of each specimen in the same panel position. Figure 6.1 illustrates the results of thickness swelling tested in 12 positions in each panel of X50-1,

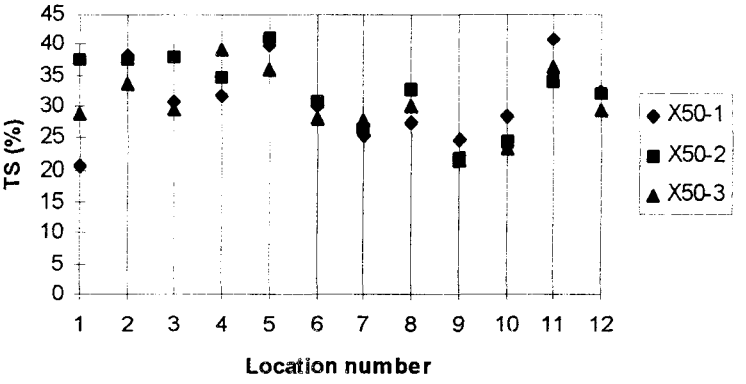

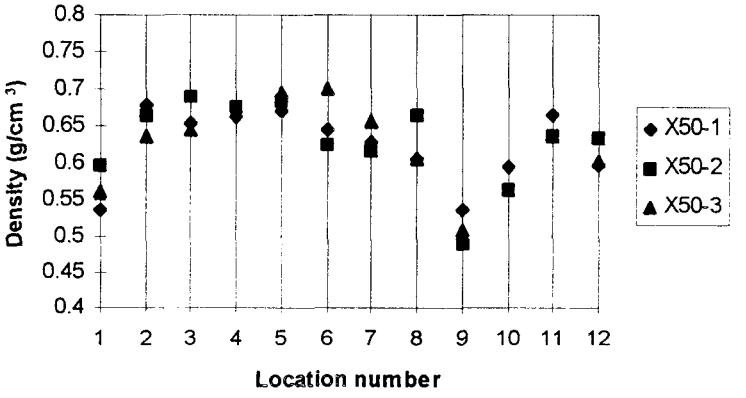

FIG. 6.1. Thickness swelling of three replicates of X50 pattern in 12 positions. FIG. 6.2. Density of the specimens for thickness swelling test of X50 pattern.

X50-2 and X-50-3. Figure 6.2 displays the corresponding real density in 12 positions of the above three replicates of pattern X50. As can be seen from the two figures, the repeatability of both panel property and density is reasonably good. This gives confidence to use robot as a tool in the future simulation study.

CONCLUSIONS

Based on the results of this research, the following conclusions can be drawn:

1. Robot system can be a very effective tool to link a simulation program with an experimental mat. The repeatability of the structure and performance of all replicates for each pattern are good, which shows promise to employ this new tool in the future study.
2. The validity of simulation program *MAT* for panel HDD analysis is demonstrated.
3. Face to core ratio and core structure have strong influence on bending MOE along

the face alignment, but their roles in determining the IB and TS are limited. No significant interaction effect of the two variables is found with any properties studied.

4. Considering all the information obtained in this research, the R30 structure (30% oriented face and bottom; 70% random core) is considered as the most suitable pattern among the four for future research.

ACKNOWLEDGMENTS

The authors gratefully acknowledge the financial support of the Natural Sciences and Engineering Research Council of Canada, Forestry Canada, Forintek Canada Corp. and MacMillan Boedel (CRD0164104). Gratitude is extended to Ainsworth Lumber Co. and CAE Machinery Ltd. for contributing logs and providing equipment for flaking, respectively.

REFERENCES

AVRAMIDIS, S., AND L. A. SMITH. 1989. The effect of resin content and face-to-core ratio on some properties of oriented strand board. Holzforschung 43(2):131–133.

CANADIAN STANDARDS ASSOCIATION (CSA). 1994. Standards on OSB and waferboard. CAN/CSA-0437.0-93. Rexdale, Ontario.

DAI, C., AND P. R. STEINER. 1994. Spatial structure of wood composites in relation to simulation of a randomly formed flake later network. Part 2. Modeling and simulation of a randomly formed flake layer network. Wood Sci. Technol. 28:135–146.

GEIMER, G. L. 1981. Predicting shear and internal bond properties of flakeboard. Holz Roh-Werkst. 39(10):409–415.

KELLY, M. 1977. Critical review of relationships between processing parameters and physical properties of particleboard. General Technical Report FPL-10. USDA Forest Product Lab., Madison, WI. 65 pp.

LANG, E. M., AND M. P. WOLCOTT. 1996. A model for viscoelastic consolidation of wood-strand mats. Part 1. Structural characterization of the mat via Monte Carlo simulation. Wood Fiber Sci. 28(1):100–109.

LU, C. 1995. Composite mat simulation program. Directed study report. Department of Wood Science, Univ. of British Columbia, Vancouver, BC.

MCNATT, J. D., L. BACH, AND R. W. WELLWOOD. 1992. Contribution of flake alignment to performance of strandboard. Forest Prod. J. 42(3):45–50.

SUCHSLAND, O., AND H. XU. 1991. Model analysis of flakeboard variables. Forest Prod. J. 41(11/12):55–60.

XU, W., AND P. R. STEINER. 1995. A statistical characterization of the horizontal density distribution in flakeboard. Wood Fiber Sci. 27(2):160–167.